

## Hydrolytic stability of polybenzobisoxazole and polyterephthalamide body armor

Amanda L. Forster<sup>a,\*</sup>, Pierre Pintus<sup>a</sup>, Guillaume H.R. Messin<sup>a</sup>, Michael A. Riley<sup>a</sup>, Sylvain Petit<sup>b</sup>, Walter Rossiter<sup>b</sup>, Joannie Chin<sup>b</sup>, Kirk D. Rice<sup>a</sup>

<sup>a</sup>Office of Law Enforcement Standards, Electronics and Electrical Engineering Laboratory, National Institute of Standards and Technology, Gaithersburg, MD, USA

<sup>b</sup>Building and Fire Research Laboratory, National Institute of Standards and Technology, Gaithersburg, MD, USA

### ARTICLE INFO

#### Article history:

Received 7 May 2010

Received in revised form

3 September 2010

Accepted 23 October 2010

Available online 11 November 2010

#### Keywords:

Body armor

Environmental conditioning

Viscometry

Molar mass

Hydrolysis

Poly(*p*-phenylene-2,6-benzobisoxazole)

### ABSTRACT

Previous work conducted at the National Institute of Standards and Technology (NIST) to investigate the field failures of soft body armor containing the material poly(*p*-phenylene-2,6-benzobisoxazole), or PBO, revealed that this material was susceptible to hydrolysis, and a mechanism of this hydrolysis was proposed. In this work, viscometric estimations of the molar mass of environmentally conditioned PBO are used to support a previously proposed mechanism of PBO hydrolysis. Results with PBO were compared with poly(*p*-phenylene terephthalamide), or PPTA, which has been used in body armor applications for more than 30 years. Losses in tensile strength were found to correspond to a reduction in molar mass for PBO. This indicates that chain scission due to complete hydrolysis is occurring in this material. Similar trends were observed for PPTA, but the relationship between molar mass reduction and losses in tensile strength was not as evident for this material. Confocal microscopy, mechanical properties measurements, and molecular spectroscopy are used to further investigate the degradation of both PBO and PPTA.

Published by Elsevier Ltd.

### 1. Introduction

In the summer of 2003, failures of soft body armor containing the material poly(*p*-phenylene-2,6-benzobisoxazole), or PBO, led to the 2003 US Attorney General's Safety Initiative to study this material. The National Institute of Justice (NIJ) and the National Institute of Standards and Technology's (NIST) Office of Law Enforcement Standards (OLES) have been partners in the development of performance standards for body armor since the 1970's. In response to the 2003 Attorney General's Initiative, OLES and NIST worked closely with NIJ to examine issues concerning PBO durability in the field and published several reports [1–3] documenting the degradation of PBO fiber in elevated conditions of moisture and temperature. Other work previously published at NIST documented a detailed examination of the failure of an officer's PBO armor in the field [4]. Two key observations from this study were that yarns extracted from the officer's armor showed a 32% reduction in tensile strength when compared with yarns extracted from a new armor, and that infrared analysis of yarns from the officer's vest showed evidence of degradation in the molecular structure of PBO (Fig. 1). Further studies at NIST

examined the degradation of PBO armors under controlled laboratory conditions [5]. A crucial finding from these studies was that PBO fibers degrade when exposed to elevated conditions of moisture and temperature (50 °C, 60% RH), but are stable when exposed to elevated temperature (55 °C) in a dry environment. This work resulted in a proposed mechanism of PBO hydrolysis, supported by previous work on hydrolysis of benzoxazoles and oxazoles [6–17], which could lead to chain scission, and a subsequent molar mass reduction, as depicted in Fig. 3 [5]. To further investigate this mechanism, a study was designed to examine hydrolytic changes in the tensile strength and molar mass of PBO and poly(*p*-phenylene terephthalamide), or PPTA (Fig. 2). A proposed mechanism for the hydrolysis leading to chain scission of PPTA is given in Fig. 4 [18,19]. The main purpose of this study is to ascertain whether or not the degradation of PBO due to environmental conditioning results in complete (leading to chain scission, Fig. 3, Step 3.) or partial hydrolysis (ceasing at the ring opening step, Fig. 3, Step 2.). This study involved controlled exposures of both PPTA and PBO fibers to hydrolytic conditions. Samples were taken periodically and analyzed using tensile testing to determine their residual tensile strength, molecular spectroscopy for evidence of hydrolysis, and viscometry for a qualitative analysis of changes in molar mass. Confocal microscopy was performed on unexposed and exposed fibers to look for obvious changes in the fiber surface. These results of these studies are presented herein.

\* Corresponding author. Tel.: +1 3019755632.

E-mail address: [amanda.forster@nist.gov](mailto:amanda.forster@nist.gov) (A.L. Forster).

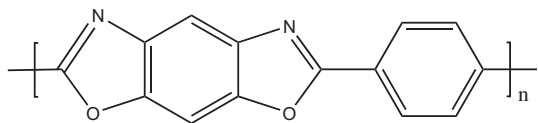


Fig. 1. Chemical structure of PBO [4,20].

## 2. Experimental

### 2.1. Environmental conditioning

In daily use, soft body armor (SBA) is exposed to environmental conditions near body temperature and humidities near complete saturation (due to perspiration of the wearer). In an effort to accelerate degradation at the defined wear temperature of 35 °C, a temperature of 70 °C was selected for the environmental conditions used in this study. A relative humidity of 90% was used to provide complete saturation of the ballistic fibers within the armor. Further details of the selection of these conditions are the subject of another publication [24]. In addition to environmental degradation, mechanical wear must also be considered as a degradation factor for SBA. A conservative analysis estimates that a body armor user might bend at the waist (e.g., when entering or exiting a vehicle) 4 times per hour, 40 h per week, 50 weeks per year, which could result in 8000 folding cycles per year, or 40,000 folding cycles over 5 years. Realistically, almost any movement a wearer makes results in some type of bend or fold in the armor, which could add up to many thousands of cycles per year [25]. Significant work has been devoted to this area by Holmes and co-workers [26]. Tumbling at a speed of 0.52 rad/s (5 rpm) was selected to provide artificial mechanical wear because it can simulate the folding damage of interest and can be performed in an environmental chamber.

### 2.2. Sample descriptions

Environmental conditioning was performed using the apparatus specified in Section 5 of NIJ Standard–0101.06 [27] for combined tumbling and environmental exposure. Sixteen SBA panels (each SBA consists of 2 armor panels, equivalent to one front and one back) were environmentally conditioned, of which 10 were used for this study. Five of the SBA panels were constructed of 20 layers of plain woven 500 denier PBO, with 26 yarns per inch in the horizontal direction and 26 yarns per inch in the vertical direction. The layers of fabric were stitched together in two packs of 10 layers each with a 2.54 cm (1 in) diagonal quilt stitch to form the ballistic package. This ballistic package was then encased in a sewn vapor-permeable fabric cover and inserted into a lightweight poly-cotton carrier to form an armor panel. Another 5 SBA panels were constructed of 25 layers of plain woven 500 denier PPTA, with 24 yarns in the horizontal direction and 24 yarns in the vertical direction. The layers of fabric were quilted together in one package with a 3.18 cm (1.25 in) diagonal stitch to form the ballistic package. This ballistic package was then encased in a standard water-repellent treated nylon fabric cover and inserted into a medium-weight poly-cotton carrier to form each armor panel.

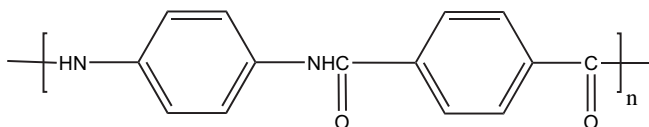


Fig. 2. Chemical structure of PPTA [18,20,21].

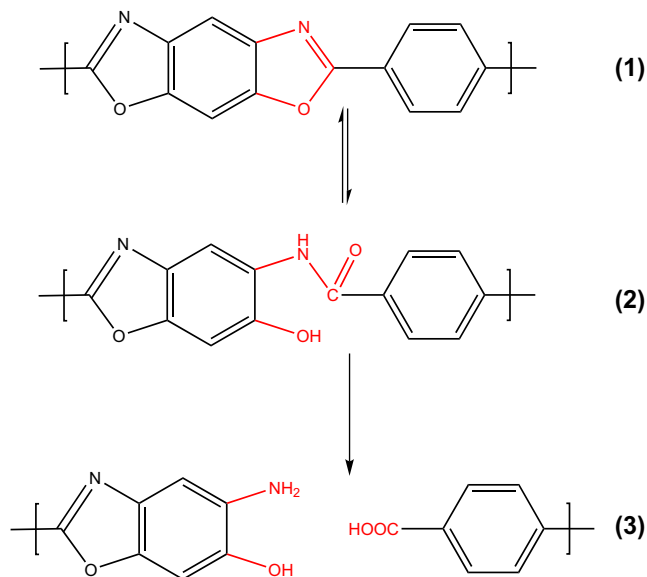


Fig. 3. Proposed mechanism of hydrolysis for PBO with chain scission [4–17,22,23].

### 2.3. Analytical methods

#### 2.3.1. Extracted yarn tensile testing

To obtain yarn mechanical properties, tensile testing of yarns extracted from each SBA panel were performed in accordance with ASTM D2256-02: “Standard Test Method for Tensile Properties of Yarn by the Single-Strand Method,” using an Instron<sup>1</sup> Model 4482 test frame equipped with a 91 kg (200 lb) load cell, and pneumatic yarn and cord grips. The jaw separation was 7.9 cm (3.1 in) and the cross-head speed was 2.3 cm/min (0.9 in/min). In this study, each yarn was nominally 38.1 cm (15 in) long, and was twisted to 60 turns on a custom designed yarn twisting device. The twist was maintained on each yarn during insertion into pneumatic yarn and cord grips. Strain measurements were made with an Instron non-contacting Type 3 video extensometer in conjunction with black foam markers placed approximately 2.5 cm apart in the gage section of the yarn. Ten to twelve replicates from each SBA panel were tested to failure. The standard uncertainty of these measurements is typically  $\pm 3\%$ , however the error bars generated for plots presented herein represent the relative standard deviation of the yarn breaking strength, which is in some cases higher than 3%.

#### 2.3.2. Fourier transform infrared analysis

Infrared analysis was carried out using a Bruker Vertex 80 Fourier Transform Infrared (FTIR) Spectrometer equipped with a mercury-cadmium-telluride (MCT) detector and a Smiths Detection Durascope attenuated total reflectance (ATR) accessory. Air, dried by passage through a standard FTIR purge gas generator, was used as the purge gas. Consistent pressure on the yarns was applied using the force monitor on the Durascope. FTIR spectra were recorded at a resolution of 4  $\text{cm}^{-1}$  between 3500  $\text{cm}^{-1}$  and 700  $\text{cm}^{-1}$  and averaged over 128 scans. Three different locations on each yarn were analyzed. Spectral analysis, including spectral subtraction, was carried out using a custom software program developed in the

<sup>1</sup> Certain commercial equipment, instruments, or materials are identified in this paper in order to specify the experimental procedure adequately. Such identification is not intended to imply recommendation or endorsement by the National Institute of Standards and Technology, nor is it intended to imply that the materials or equipment identified are necessarily the best available for this purpose.

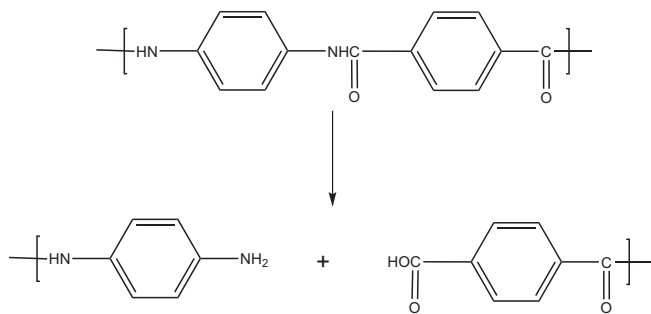


Fig. 4. Proposed mechanism of hydrolysis for PPTA [18,22,23].

Building and Fire Research Laboratory's Polymeric Materials Group at NIST. All spectra were baseline corrected and normalized using the aromatic C–H deformation peak at  $848\text{ cm}^{-1}$  for PBO and  $820\text{ cm}^{-1}$  for PPTA. Standard uncertainties associated with this measurement are typically  $\pm 4\text{ cm}^{-1}$  in wavenumber and  $\pm 1\%$  in peak intensity.

### 2.3.3. Dilute solution viscometry

PBO is only soluble in strong anhydrous acids such as sulfuric acid (SA), chlorosulfonic acid (CSA), and methanesulfonic acid (MSA) [28]. Previous viscometry work has been published using MSA as a solvent for PBO, so this solvent was selected for the purposes of this study for comparison to literature [28,33–37]. All acid solvents were purchased in their anhydrous form and were used as received. All glassware and fibers were dried using a flow of dry nitrogen, placed in an oven at  $35\text{ }^{\circ}\text{C}$  for several hours, and stored in a desiccator filled with dry silica gel prior to use to minimize contamination of the samples with water. For the PBO, a stock solution was prepared at a concentration of  $1\text{ mg/mL}$ , from which dilutions were made to obtain samples at concentrations of  $0.01\text{ g/dL}$ ,  $0.03\text{ g/dL}$ ,  $0.05\text{ g/dL}$ ,  $0.07\text{ g/dL}$ , and  $0.1\text{ g/dL}$ . For PPTA, a stock solution was prepared at a concentration of  $2\text{ mg/mL}$ , from which dilutions were made to obtain samples at concentrations of  $0.02\text{ g/dL}$ ,  $0.10\text{ g/dL}$ , and  $0.20\text{ g/dL}$ . All sample solutions were purged with dry nitrogen during dissolution. PBO solutions were prepared at  $150\text{ }^{\circ}\text{C}$  on a stirring hot plate and the PPTA solutions were prepared at room temperature on a stirring hotplate. All solutions were prepared and consumed in the same day to reduce the potential for contamination with water. Prepared solutions were purged with dry nitrogen and stored in a desiccator when not in use. Kinematic viscosities were measured using Cannon capillary viscometers in a thermostatic bath (Koehler K23376) at  $25\text{ }^{\circ}\text{C} \pm 0.05\text{ }^{\circ}\text{C}$ . The viscometer elution times were in the range of  $241\text{--}471\text{ s}$ . The standard deviation is less than the viscometer elution times ( $0.3\%$ ).

### 2.4. Laser scanning confocal microscopy

A Zeiss Model LSM510 reflection laser scanning confocal microscope (LSCM) was employed to characterize the surface morphology. The incident laser wavelength was  $543\text{ nm}$ . By moving the focal plane in the  $z$ -direction, a series of single images (optical slices) can be stacked and digitally summed over the  $z$ -direction to obtain a 3-D image. All images were collected using the  $150\times$  objective and a  $z$ -direction step size of  $0.1\text{ }\mu\text{m}$ .

## 3. Results and discussion

### 3.1. Hydrolysis of PBO and PPTA

Previous studies [4,5] have shown that oxazole ring opening is a major indicator of hydrolysis in PBO. Through the use of difference

spectra, where the infrared spectrum taken from the unconditioned sample (in this case, from a new vest) is subtracted from the spectra of yarns removed from the vest at different stages of environmental conditioning, the evolution of changes in the chemical structure can be studied [4,5,29–31]. Negative peaks in difference spectra are attributed to the loss of existing chemical structure, and positive peaks are indicative of the formation of new chemical structure [29–31]. Benzoxazole ring opening is identified by the loss of peaks attributed to the vibrations associated with the benzoxazole ring at  $1496\text{ cm}^{-1}$ ,  $1362\text{ cm}^{-1}$ ,  $1056\text{ cm}^{-1}$ , and  $914\text{ cm}^{-1}$ , and by the formation of a peak at  $1650\text{ cm}^{-1}$  attributed to a carbonyl from amide or carboxylic acid, which are potential products of oxazole ring opening [5]. Infrared difference spectra of PBO taken over the course of the exposure study are shown in Fig. 5. The PBO difference spectra show marked reductions in the peaks at  $1498\text{ cm}^{-1}$ ,  $1369\text{ cm}^{-1}$ ,  $1060\text{ cm}^{-1}$ , and  $919\text{ cm}^{-1}$ , all of which are attributed to oxazole ring opening [5]. (Differences in the wavenumbers between the previous study and the current study are attributed to the use of two different spectrometers.) As previously mentioned, standard uncertainties associated with this measurement are typically  $4\text{ cm}^{-1}$  in wavenumber and  $1\%$  in peak intensity, so the slight shift in wavenumbers for the difference spectra may be due to variations in the individual spectra used to create the difference spectrum [29–32]. The increase in the carbonyl peak at  $1650\text{ cm}^{-1}$  indicates the formation of a carbonyl-containing species such as an amide or carboxylic acid, as expected by the mechanism shown in Fig. 3. This increase is similar to that seen in previous studies [5,24].

The PPTA difference spectra in Fig. 6 shows negative peaks with positions corresponding to the original amide I peak at  $1643\text{ cm}^{-1}$  and amide II peak at  $1502\text{ cm}^{-1}$ . A new broad peak is observed at  $3300\text{ cm}^{-1}$ , which is attributed to a combination of amine N–H stretching and carboxylic acid OH stretching. New peaks are also observed at  $1562\text{ cm}^{-1}$  and  $1420\text{ cm}^{-1}$  that are attributed to carboxylate ion stretching. This evidence points to the hydrolysis of the main chain amide group to amine and carboxylic acid as previously shown in Fig. 4.

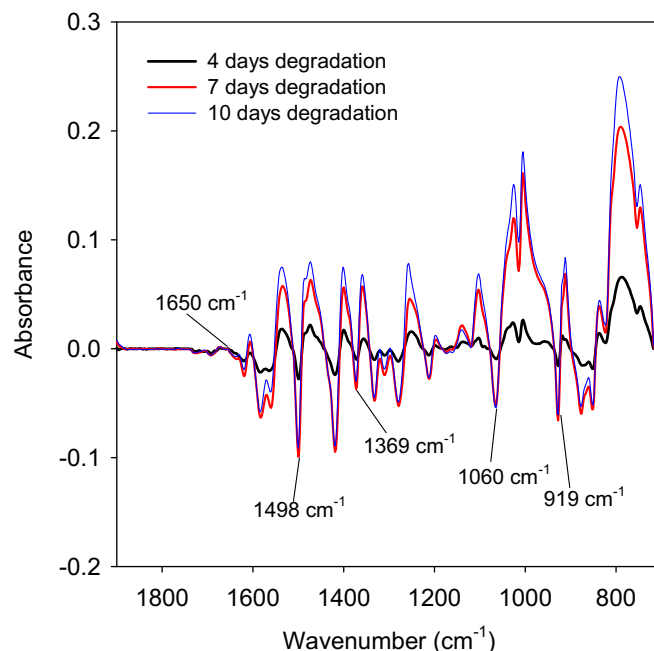


Fig. 5. Difference ATR-FTIR spectra of PBO during environmental conditioning, referenced to undegraded samples.

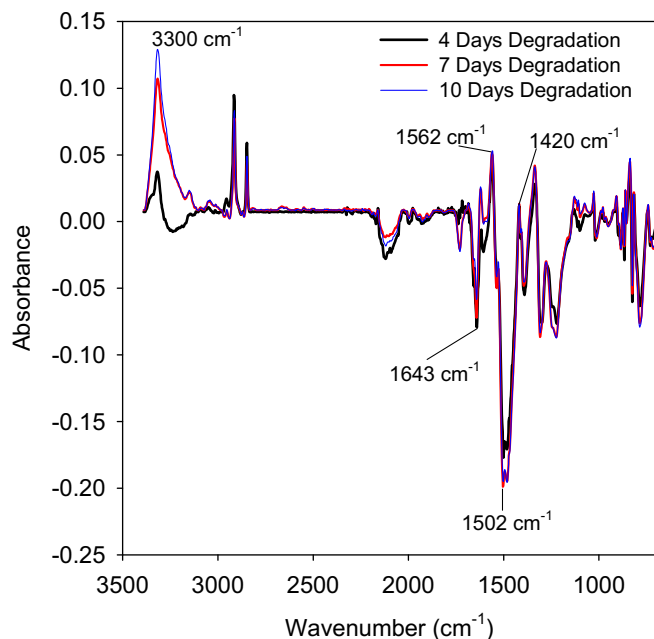


Fig. 6. Difference ATR-FTIR spectra of PPTA during environmental conditioning, referenced to undegraded samples.

### 3.2. Intrinsic viscosity analysis

Previous work has provided a detailed analysis of the application of the Mark–Houwink equation to polymers such as PBO and PPTA [21,28,33–38]. Several papers have focused on the effect of ionic strength (varied by the addition of water and salts such as  $\text{CH}_3\text{SO}_3\text{Na}$ ,  $\text{LiF}_3\text{CSO}_3$ , or  $\text{Li}_2\text{SO}_4$ ) on the solution properties of these polymers [33,35,37]. Roitman has shown for low polymer solution concentrations (less than 0.01 g/dL), small amounts of ionizable solutes (such as water) in concentrations of less than 0.1 M can cause anomalous viscosity behavior [33]. In an effort to avoid this problem in this study, the minimum polymer concentration used was 0.01 g/dL.

A discussion of the necessary calculations to perform intrinsic viscosity analysis of polymer solutions to estimate molar mass can be found in many basic polymer science textbooks [39–41]. For completeness of this work, a brief discussion of the equations used in this analysis is given here.

The efflux time of each polymer solution in the viscometer,  $t$ , was compared to the efflux time of the pure solvent,  $t_0$ , to obtain the relative viscosity,  $\eta_{rel}$ , as shown by Equation (1), and the specific viscosity,  $\eta_{sp}$ , as shown by Equation (2) [39,40].

$$\eta_{rel} = \frac{t}{t_0} \quad (1)$$

$$\eta_{sp} = \frac{t - t_0}{t_0} \quad (2)$$

The reduced viscosity,  $\eta_{red}$ , is determined by dividing the specific viscosity,  $\eta_{sp}$ , by the concentration of the polymer solution,  $c$ , as shown by Equation (3) [39,40].

$$\eta_{red} = \frac{\eta_{sp}}{c} \quad (3)$$

The inherent viscosity,  $\eta_{inh}$ , is determined by dividing the natural log of the relative viscosity,  $\eta_{rel}$ , by the concentration of the polymer solution,  $c$ , as shown by Equation (4) [39,40].

$$\eta_{inh} = \frac{\ln \eta_{rel}}{c} \quad (4)$$

The reduced viscosity,  $\eta_{red}$ , was plotted as a function of concentration and the y-intercept of this plot is taken as the intrinsic viscosity,  $[\eta]$ , which can be used to estimate molar mass. This process was repeated with the inherent viscosity,  $\eta_{inh}$ , to obtain two different estimates for intrinsic viscosity,  $[\eta]$ . The values of the y-intercepts were taken as the intrinsic viscosities as shown by Equations (5) and (6) [39,40].

$$[\eta_{red}] = k'[\eta]^2 c + [\eta] \quad (5)$$

$$[\eta_{inh}] = k''[\eta]^2 c + [\eta]^2 c + [\eta] \quad (6)$$

Estimates of the intrinsic viscosity via these two methods agreed to within 0.4 g/dL, except for the undegraded PBO sample, which only had agreement to within 1.5 g/dL. Values of the intrinsic viscosity estimated by each equation are presented in Table 1 for PBO and PPTA.

Fig. 7 shows representative viscosity data obtained for PBO which had been environmentally conditioned for 4 d and Fig. 8 shows representative data for PPTA which had been environmentally conditioned for 10 d.

For PBO, the highly conjugated structure of the polymer chain from the extended delocalization of  $\pi$  electrons over the benzobisoxazole and phenyl rings results in a very rigid molecular structure [28]. The only possible conformational flexibility is attributed to rotation of bonds between the phenyl ring and oxazole ring [28]. The high orientation of PPTA and PBO fibers is typically ascribed to the formation of a nematic phase at sufficient concentration, which allows the rod-like molecules to orient themselves with respect to the fiber axis during fiber formation [33,42–44]. The average of the two calculated intrinsic viscosities was used to estimate the weight average molar mass using the Mark–Houwink equation for PBO, Equation (7) [28,37], and PPTA, Equation (8) [37,38].

$$[\eta] = 2.27 \times 10^{-7} \overline{M}_w^{1.8} \quad (7)$$

The Mark–Houwink exponent of 1.8 is an indication of the high molecular rigidity of PBO. For comparison, this exponent is 1.0 for semi-rigid polymers, and for an ideal random coil polymer under  $\theta$  conditions it is 0.5. The value of 1.09 for Kevlar reflects its slightly more flexible molecular structure [28].

$$[\eta] = 8.0 \times 10^{-5} \overline{M}_w^{1.09} \quad (8)$$

Equations (7) and (8) were used to calculate an estimated weight average molar mass for samples extracted from both armors during the environmental conditioning experiment. The baseline (undegraded) PBO sample has a molar mass of approximately 26,000 g/mol, which is comparable to the 28,650 g/mol previously reported by Gupta [36]. The goal of this study was to examine the relative changes in molar mass during environmental conditioning instead of attempting to make an absolute measurement of molar mass, so it was determined that this estimate was acceptable for

Table 1  
Estimation of intrinsic viscosity with  $\eta_{red}$  and  $\eta_{inh}$  for PBO and PPTA.

Environmental conditioning (d)	PBO $[\eta]$ est. by $\eta_{red}$	PBO $[\eta]$ est. by $\eta_{inh}$	PPTA $[\eta]$ est. by $\eta_{red}$	PPTA $[\eta]$ est. by $\eta_{inh}$
0	18.577	19.998	8.62	9.01
4	15.504	15.535	7.47	7.60
7	11.408	11.786	5.95	6.01
10	7.597	7.637	4.96	4.96

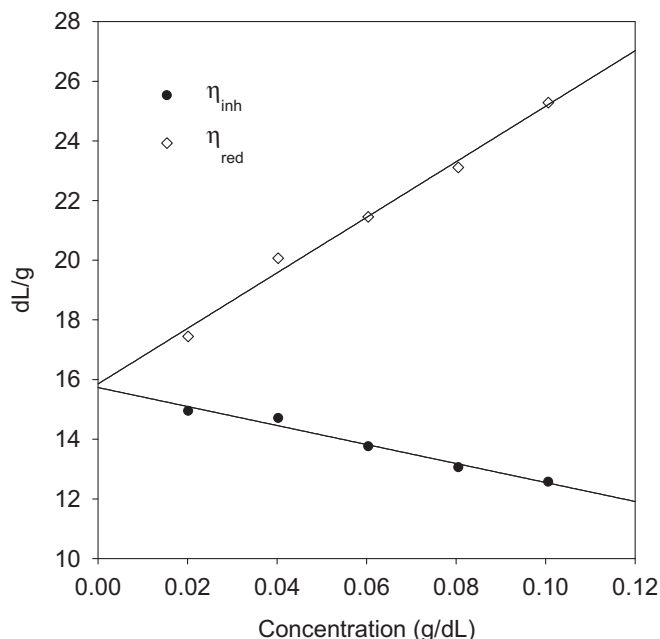


Fig. 7. Representative viscosity data for PBO which had been environmentally conditioned for 4 d.

this qualitative technique. Over the course of the environmental conditioning, the PBO sample degraded to an approximate molar mass of 15,000 g/mol. The baseline (undegraded) PPTA sample molar mass was calculated to be approximately 42,000 g/mol. This value was verified by a PPTA manufacturer [45] to be reasonable, but is considerably higher than that reported in the literature [21]. After 10 d of environmental conditioning, the molar mass of the PPTA sample was reduced to approximately 25,000 g/mol. Full details of these results are presented in Table 2.

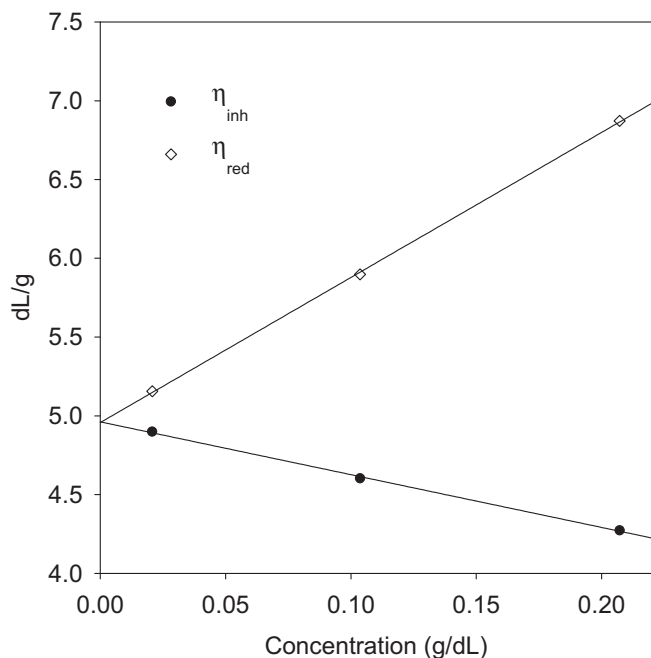


Fig. 8. Representative viscosity data for PPTA which had been environmentally conditioned for 10 d.

Table 2

Estimation of the reduction of weight average molar mass for PBO and PPTA with environmental conditioning.

Environmental conditioning (d)	PBO (g/mol)	PPTA (g/mol)
0	26.157	42.241
4	22.746	36.579
7	19.161	29.595
10	15.169	24.926

### 3.3. Comparison of molar mass reduction with tensile strength reduction

After 10 d of environmental conditioning, the PBO sample had a tensile strength retention of approximately 68%. The PPTA sample tumbled in the environmental conditioning environment had a tensile strength retention of approximately 85%. This strength loss in the PPTA armor was greater than that observed in previous studies [24]. Error bars represent the relative standard deviations.

In an effort to more readily compare the estimated reduction in molar mass with the extracted yarn tensile testing results for PBO and PPTA the molar masses were also converted to a percentage of the original value. This conversion of the data allowed for the determination of the percent residual tensile strength and the percent residual molar mass, which are plotted as a function of environmental conditioning time in Figs. 9 and 10. This approach revealed a correspondence between the reduction in molar mass and the reduction in tensile strength with increased environmental conditioning time. To further examine this phenomenon, for PBO, residual tensile strength was plotted against residual molar mass, and a least squared linear fit yielded an  $R^2$  value of 0.97 and a slope of  $a=0.75$ , suggesting a correspondence between residual tensile strength and residual molar mass. The reduction in molar mass, which would be indicative of chain scission, may support the hypothesis that PBO fully undergoes chain scission during exposure to elevated conditions of temperature, moisture, and mechanical damage, as opposed to simply undergoing the benzoxazole ring opening step of the hydrolysis reaction as shown in structure (2) of

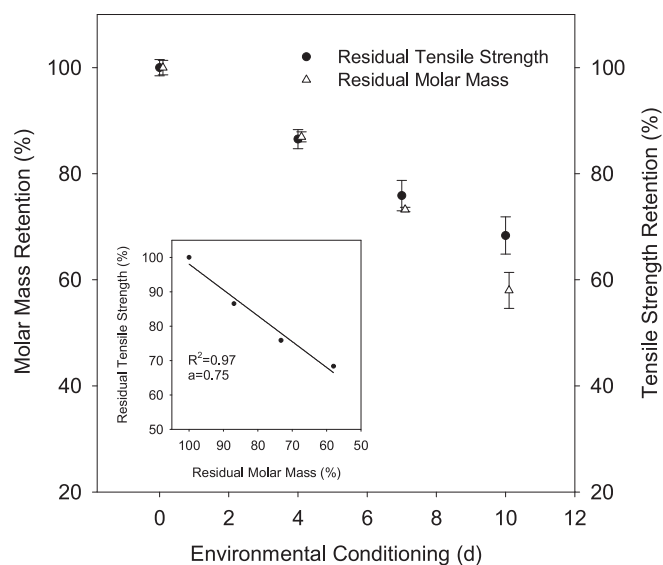
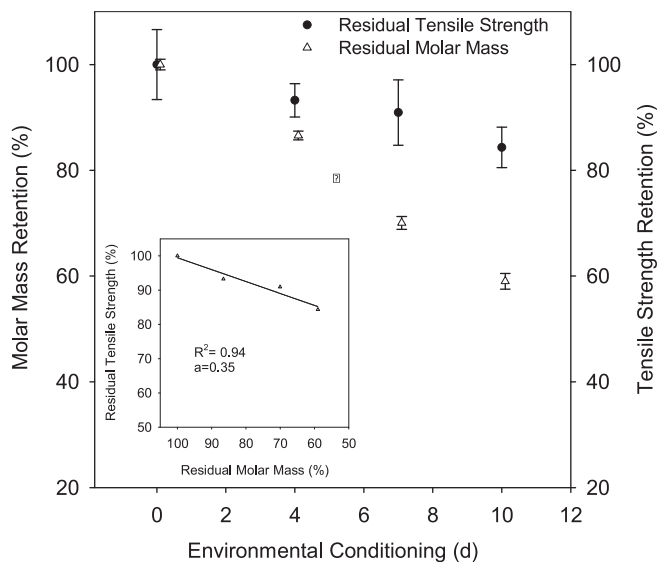
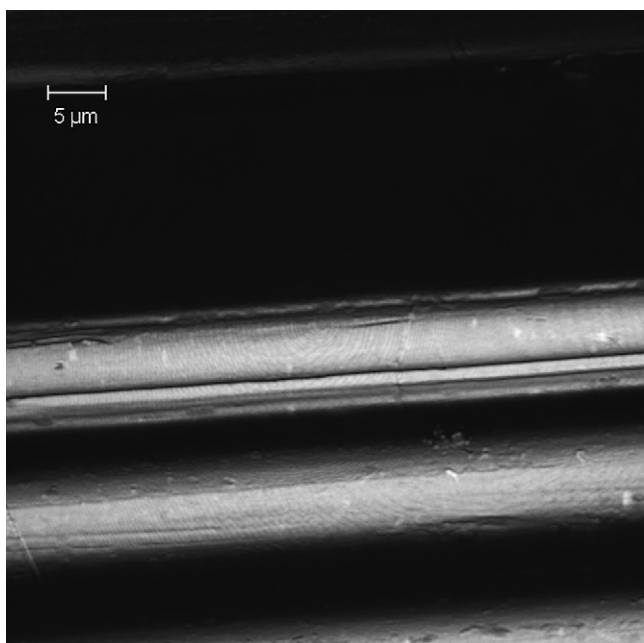


Fig. 9. Comparison of residual tensile strength with residual molar mass for PBO. The error bars represent the relative standard deviation of the mean yarn breaking strength or mean molar mass. Residual molar mass points are offset horizontally for clarity of presentation.



**Fig. 10.** Comparison of residual tensile strength with residual molar mass for PPTA. The error bars represent the relative standard deviation of the mean yarn breaking strength or mean molar mass. Residual molar mass points are offset horizontally for clarity of presentation.

**Fig. 3**, which would give a fiber with a structure similar to PPTA. While the overall downward trend is supported with this same analysis for PPTA, when a linear polynomial fit was applied to the data, the  $R^2$  value was 0.94 and the slope was  $a=0.35$ , again indicating a correspondence between the reduction in molar mass and the reduction in tensile strength. However, the sensitivity of this relationship is different for PPTA. Future work will separate the mechanical and environmental degradation conditions in an effort to better understand their individual roles in the environmental conditioning of PBO and PPTA fibers and to fully answer the question of how hydrolysis progresses in PBO.



**Fig. 11.** Confocal 2D projection of undegraded PBO fiber.

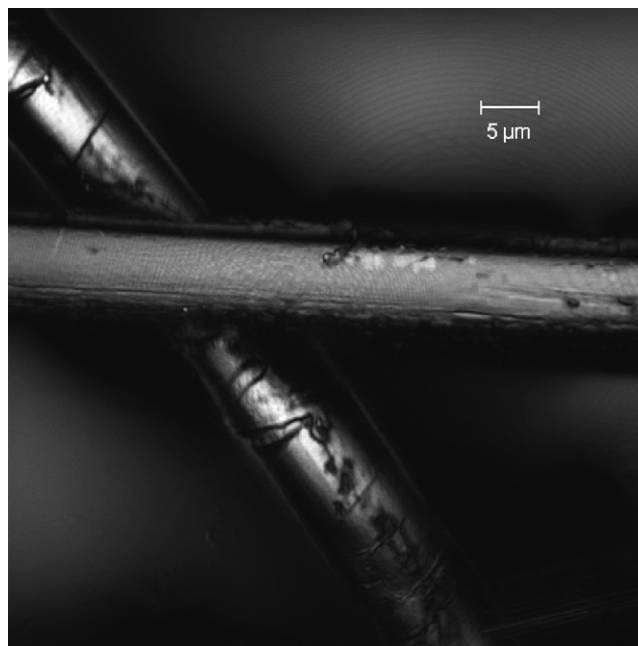


**Fig. 12.** Confocal 2D projection of PBO fiber environmentally conditioned for 10 d. Note the kink-bands in the lower fiber and the pitting in the upper fiber.

#### 3.4. Microscopic examination of fiber surface

It is possible that the observed reduction in molar mass and tensile strength can be attributed to the polymer being abraded due to mechanical action as the body armor fabric undergoes tumbling. To minimize this possibility, the yarns used in testing were removed from the inner layers of the body armors. This practice, combined with the fact that the armor was tumbled inside of two protective layers (the carrier and the armor panel cover), and

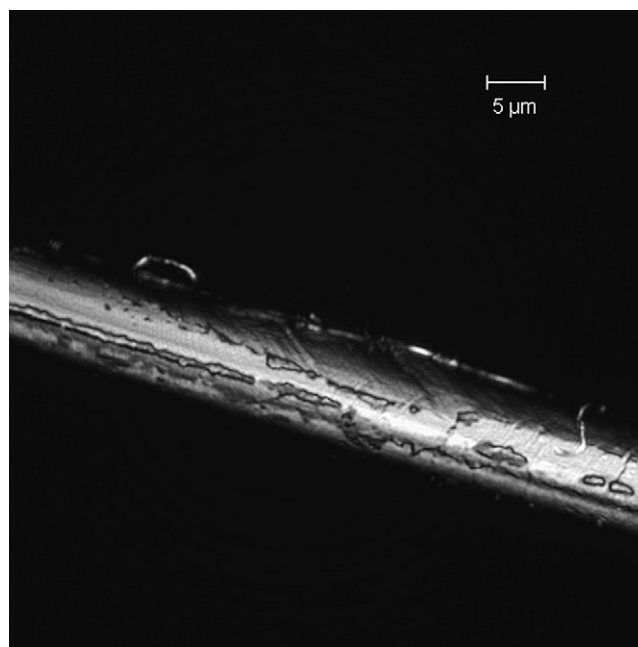


**Fig. 13.** Confocal 2D projection of undegraded PPTA fiber. Note the shiny, reflective surface of the smooth undegraded fiber. Darker spots on the image are likely due to lubricants from processing.

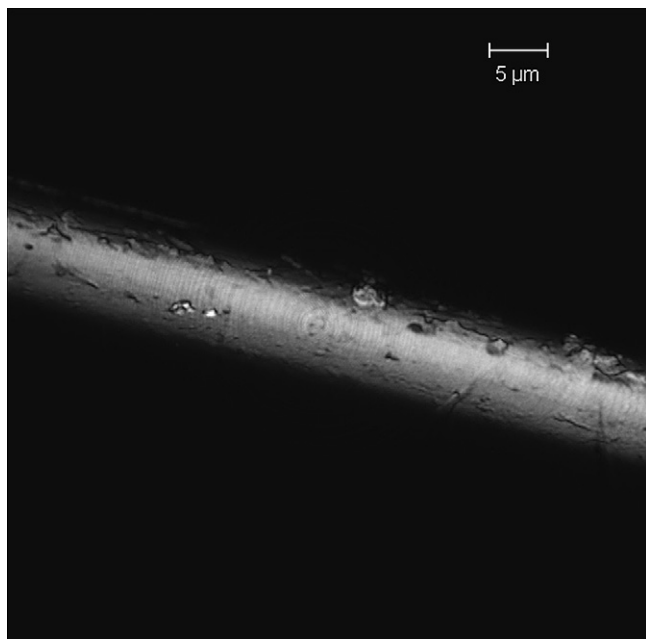


**Fig. 14.** Confocal 2D projection of PPTA fiber environmentally conditioned for 10 d. Note the dull surface of the degraded fiber. Darker spots are indicative of pitting in the surface.

stitched together to minimize layer-to-layer friction, should reduce the effect of abrasion on the results. In order to further examine the effect of abrasion, confocal microscopy was used to examine fibers before and after environmental conditioning (Figs. 11 and 12). There is some evidence of additional formation of pits and kink-bands on the surface of the degraded samples. Similar confocal images were obtained in a previous study and these changes were attributed to hydrolysis and chemical exposure [32]. Confocal images of PPTA before and after degradation (Figs. 13 and 14) show an increase in surface smoothness (possibly due to abrasion) after environmental conditioning, similar to that seen in other studies where fibers were intentionally abraded [25]. Images observed in previous microscopy studies on PPTA fibers after exposure to artificial sweat and cleaning chemicals are also similar [32]. A detailed discussion of the use of confocal microscopy to examine the surface of fibers exposed to hydrolytic and mechanically abrasive conditions will be the subject of a future paper.

#### 4. Conclusions

Fibers such as PBO and PPTA have been used in soft body armor applications due to their high strength properties. However, these fibers can be sensitive to environmental degradation via elevated temperature, humidity, and mechanical damage. These conditions were simulated through environmental conditioning. A comparison of the residual tensile strength with residual molar mass for environmentally conditioned PBO indicated that the degradation of PBO fibers may be due to hydrolytic chain scission of this polymer. A reduction in both tensile strength and molar mass was also observed for environmentally conditioned PPTA fibers, but the sensitivity of this relationship is different for this material as compared to PBO.

#### 5. Future work

In order to better understand the behavior of the PPTA fibers, dilute solution viscometry experiments are planned to examine

fibers which were exposed to an environment of elevated temperature and humidity, without mechanical damage, and fibers which were exposed to mechanical damage in an ambient environment. Additional experiments are planned to evaluate light scattering as a comparison method for measurement of molar mass. Finally, a forthcoming publication will examine the use of confocal microscopy to examine fiber surfaces after exposure to hydrolytic and mechanically damaging conditions.

#### Acknowledgments

The authors gratefully acknowledge financial support for this research effort provided by the National Institute of Justice under Interagency Agreement Number 2003-IJ-R-029. The authors would also like to thank Minshon Chiou and Vlodex Gabara of E. I. du Pont de Nemours and Company for helpful discussions.

#### References

- [1] Status report to the attorney general of body armor safety initiative testing and activities, NIJ special report, 2004.
- [2] Supplement 1: status report to the attorney general of body armor safety initiative testing and activities, NIJ special report, 2004.
- [3] Third status report to the attorney general on the body armor safety initiative testing and activities, NIJ special report, 2005.
- [4] Chin J, Byrd E, Forster AL, Gu X, Nguyen T, Scierka S, et al. Chemical and physical characterization of poly (*p*-phenylene-2,6-benzobisoxazole) fibers used in body armor. NISTIR 2006;7237.
- [5] Chin J, Byrd E, Clerici C, Oudina M, Sung L, Forster AL, et al. Chemical and physical characterization of poly (*p*-phenylene-2,6-benzobisoxazole) fibers used in body armor: temperature and humidity aging. NISTIR 2007;7373.
- [6] Wiley RH. The chemistry of the oxazoles. *Chem Rev* 1945;37:401–42.
- [7] Cornforth JW. Heterocyclic compounds. 5th ed. New York: John Wiley and Sons; 1957.
- [8] Turchi IJ. Oxazoles. New York: John Wiley and Sons; 1986.
- [9] Palmer DC, Venkataraman S. Chemistry of heterocyclic compounds, oxazoles: synthesis, reactions, and spectroscopy, part A. Hoboken, New Jersey: Wiley-Interscience; 2003.
- [10] Albert A. Heterocyclic chemistry: an introduction. Fair Lawn, New Jersey: Essential Books; 1959.
- [11] Albert A. Heterocyclic chemistry: an introduction. London: The Athlone Press; 1968.
- [12] Badger GM. The chemistry of heterocyclic compounds. New York: Academic Press; 1961.
- [13] Acheson RM. An introduction to the chemistry of heterocyclic compounds. New York: Interscience Publishers; 1967.
- [14] Boyd GV. Comprehensive heterocyclic chemistry: the structure, reactions, synthesis and uses of heterocyclic compounds. Oxford: Pergamon Press; 1984.
- [15] Jackson PF, Morgan KJ, Turner AM. Studies in heterocyclic chemistry part IV: kinetics and mechanisms for the hydrolysis of benzoxazoles. *J Chem Soc Perk Trans 2* 1972;11:1582–7.
- [16] Goetz JR. Hydrolysis of 2-methylbenzoxazole to 2-hydroxyacetanilide. *Tex J Sci* 1972;24:261.
- [17] Hegedus LS, Odle RR, Winton PM, Weider PR. Synthesis of 2,5-disubstituted 3,6-diamino-1,4-benzoquinones. *J Org Chem* 1982;47:2607–13.
- [18] Morgan RJ, Butler NL. Hydrolytic degradation mechanism of Kevlar 49 fibers when dissolved in sulfuric acid. *Polym Bull* 1992;27:689–96.
- [19] Chatzi EG, Tidrick SL, Koenig JL. Characterization of the surface hydrolysis of Kevlar-49 fibers by diffuse reflectance FTIR spectroscopy. *J Polym Sci Pol Phys* 1988;26:1585–93.
- [20] Odian G. Principles of polymerization. New York: John Wiley and Sons; 1991.
- [21] Yang HH. Kevlar aramid fiber. New York: John Wiley and Sons; 1993.
- [22] Carey FA. Organic chemistry. New York: McGraw Hill; 1993.
- [23] Wade LG. Organic chemistry. Englewood Cliffs, New Jersey: Prentice-Hall; 1991.
- [24] Forster AL, Rice KD, Riley MA, Messin GHR, Petit S, Clerici C, et al. Development of soft armor conditioning protocols for NIJ standard-0101.06: analytical results. NISTIR 2009;7627.
- [25] Forster AL, Chin J, Gundlach M. Effect of bending and mechanical damage on the physical properties of poly(*p*-phenylene-2,6-benzobisoxazole)(PBO) fiber. *Abstr Pap Am Chem S*; 2006. 274-POLY:231.
- [26] Holmes GA, Kim JH, Ho DL, McDonough WG. The role of folding in the degradation of ballistic fibers. *Polym Composites* 2010;31:879–86.
- [27] Ballistic resistance of personal body armor. NIJ Standard-0101.06; 2008.
- [28] Hu XD, Jenkins SE, Min BG, Polk MB, Kumar S. Rigid-rod polymers: synthesis, processing, simulation, structure, and properties. *Macromol Mater Eng* 2003;288:823–43.
- [29] Martin J, Nguyen T, Byrd E, Dickens B, Embree N. Relating laboratory and outdoor exposures of coatings: I. Cumulative damage model and laboratory experiment apparatus. *Polym Degrad Stab* 2002;75:193–210.

- [30] Nguyen T, Martin J, Byrd E, Embree N. Relating laboratory and outdoor exposures of coatings: II. Effects of relative humidity on photodegradation and the apparent quantum yield of acrylic melamine coatings. *J Coatings Tech* 2002;74:31–44.
- [31] Nguyen T, Martin J, Byrd E, Embree N. Relating laboratory and outdoor exposures of coatings: III. Effects of relative humidity on moisture-enhanced photolysis of acrylic melamine coatings. *Polym Degrad Stab* 2002;77:1–16.
- [32] Chin J, Petit S, Forster AL, Riley M, Rice K. Effect of artificial perspiration and cleaning chemicals on the mechanical and chemical properties of ballistic materials. *J Appl Poly Sci* 2009;113:567–84.
- [33] Roitman DB, Wessling RA, McAlister J. Characterization of poly(*p*-phenylene-*cis*-benzobisoxazole) in methanesulfonic acid. *Macromolecules* 1993;26:5174–84.
- [34] Shanfeng W, Gaobin B, Pingping W, Zhewen H. Viscometric study on the interactions of polymers of the poly(benzazole) family with nylon 66. *Eur Polym J* 2000;36:1843–52.
- [35] Cotts DB, Berry GC. Polymerization kinetics of rigid rodlike molecules: polycondensation of poly ([benzo(1,2-*d*:5,4-*d'*)bisoxazole-2,6-diyl]-1,4-phenylene). *Macromolecules* 1981;14:930–4.
- [36] Gupta A. Improving UV resistance of high strength fibers. Ph.D. thesis, North Carolina State University; 2005.
- [37] Wong CP, Ohnuma H, Berry GC. Properties of some rodlike polymers in solution. *J Polym Sci Polym Symp* 1978;65:173–92.
- [38] Arpin M, Strazielle C. Study of aromatic polyamides of poly[imino-1,4-phenyleneiminoterephthaloyl]-type by gel permeation chromatography. *Macromol Chem Phys* 1976;177:293–8.
- [39] Carraher C. *Polymer chemistry*. New York: Marcel Dekker; 1996.
- [40] Rubenstein M, Colby RH. *Polymer physics*. New York: Oxford University Press; 2003.
- [41] Billmeyer F. *Textbook of polymer science*. 3rd ed. New York: John Wiley and Sons; 1984.
- [42] Doi M. *Introduction to polymer physics*. Oxford: Oxford University Press; 1996.
- [43] Collins PJ. *Liquid crystals*. Princeton, NJ: Princeton University Press; 2002.
- [44] Collins PJ, Hird M. *Introduction to liquid crystals chemistry and physics*. Philadelphia: Taylor and Francis; 1997.
- [45] Gabara V. Dilute solution viscometry of Kevlar fibers. Personal Communication; 2008.